RSC Advances

PAPER

View Article Online
View Journal | View Issue

Cite this: *RSC Adv.*, 2024, **14**, 17583

Process optimization and mechanism for the selective extraction of copper(II) from polymetallic acidic solutions using a polymer inclusion membrane (PIM) with Mextral®5640H as the carrier

Shan Zhu *[a] and Jiugang Hu[b]

This study introduces a novel approach by integrating solvent extraction and polymer inclusion membrane (PIM) separation technologies to engineer an innovative PIM membrane material for the selective separation and enrichment of strategic metals, particularly copper, from polymetallic acidic solutions. The primary objectives were to streamline the technological process, reduce production costs, and enhance separation coefficients between copper and other metals. The optimal extraction conditions were determined as a mass fraction of Mextral®5640H : PVC : NPOE = 3 : 3 : 4, extraction temperature of 35 °C, and 0.9 mol L^{-1} H_2SO_4 in the stripping solution. Under these conditions, we achieved remarkable extraction efficiencies, with copper reaching 100%, and the separation coefficients between Cu^{2+} and Ni^{2+}, Co^{2+}, and Zn^{2+} exceeding 10^6. To elucidate the substantial differences in extraction performance between Cu^{2+} and the other metals (Ni^{2+}, Co^{2+}, and Zn^{2+}), we employed an integrative analytical approach that combines FT-IR spectroscopy, BET analysis, and theoretical calculations. All extracted complexes demonstrated molecular sizes compatible with PIMs, underscoring the critical role of stability and back-extraction performance in the selective extraction of these metal ions.

Received 17th March 2024
Accepted 27th May 2024

DOI: 10.1039/d4ra02032d

rsc.li/rsc-advances

1. Introduction

Copper, nickel, cobalt, and zinc, along with their compounds, play crucial roles in various aspects of the national economy, daily life, defense industry, and scientific and technological advancements, serving as key strategic resources for enhancing national strength and security.[1] In recent years, China has made significant progress in developing and utilizing these resources. The global demand for copper, nickel, cobalt, and zinc has steadily risen, with China consistently ranking first in consumption for fourteen consecutive years. In 2014 alone, the consumption reached 11.09 million tons, 910 000 tons, 37 000 tons, and 6.35 million tons, respectively, representing 41%, 48.9%, 50.3%, and 46% of the world's total.[2]

Currently, the majority of non-ferrous metal resources in China consist of low-grade oxide minerals and polymetallic ores. With the depletion of high-grade traditional mineral resources the mineral grade is declining, resulting in increased mining challenges. Consequently, the self-sufficiency rate of strategic metals like copper, nickel, cobalt, and zinc has gradually decreased, leading to a growing dependence on external resources and highlighting a supply-demand imbalance.[3,4] Therefore, it is imperative to develop sustainable methods for the extraction of precious metals from difficult-to-process mineral resources, such as symbiotic ore, associated ore, poor ore, tailings, and slag ore.[5]

As the quality of copper, nickel, cobalt, and zinc resources in China decreases over time, it becomes challenging and costly to use traditional methods to efficiently extract these valuable metals from the leaching solutions. Consequently, the leachates and raffinates obtained from processes like leaching, electroplating, and electric industries often contain a mix of target metal ions and other impurities. This makes it crucial to directly separate and concentrate target ions in hydrometallurgical raffinates.[6]

Due to the intricate nature of hydrometallurgical raffinates, there is an urgent need for a method that can selectively separate and recover valuable metal ions from various input solutions simultaneously. In addition, this approach should offer benefits such as improved separation efficiency, a shorter technological process, and significant reductions in production costs and environmental pollution.[7]

In recent decades, several methods have been used to extract and recover valuable metals from polymetallic solutions. These include chemical precipitation,[8] resin adsorption,[9] ion exchange,[10] and solvent extraction.[11–13] Among these, solvent extraction is widely applied to selectively recover and separate

[a]School of Chemistry and Materials Engineering, Liupanshui Normal University, Liupanshui 553000, China. E-mail: zhushan19890830@163.com
[b]College of Chemistry and Chemical Engineering, Central South University, Changsha 410083, China

valuable metals from complex mixtures. For example, Cheng and his colleagues[14–19] focused on the separation of precious metals using a combination of two extractants, Versatic10 and Lix63. They successfully extracted Cu^{2+}, Co^{2+}, Ni^{2+} and Zn^{2+} into the organic phase, leaving impurities in the aqueous phase.[20]

While solvent extraction has been widely used for decades to separate Cu^{2+}, Co^{2+}, and Ni^{2+} from Ca^{2+}, Mg^{2+}, Mn^{2+}, and Fe^{3+}, there are still some drawbacks. For instance, Cheng[15,21,22] and Zhu[23] achieved high separation coefficients for Ni/Co, Ni/Mn, and Co/Mn of 675, 576, and 3065, respectively, using a synergistic combination of Lix63 and Versatic10. However, the nickel stripping rate was only 32% within 5 minutes. Li[24] also discovered that the HDNNS/pyridinecarboxylate synergistic system can selectively extract copper, nickel, and cobalt from the acidic polymetallic solutions containing impurities like Ca^{2+}, Mg^{2+}, Mn^{2+}, Cr^{2+}, Fe^{3+}, Al^{3+}, *etc.* Although improving the structure of the pyridinecarboxylate carbon chain and purifying the commercial extractant HDNNS enhanced the phase separation in the HDNNS/pyridinecarboxylate co-extraction system, increasing the extraction clarification rate from 0.4 $m^3\ m^{-2}\ h^{-1}$ to 1.0 $m^3\ m^{-2}\ h^{-1}$, it still falls short of meeting the industrial design demands of 2.4 $m^3\ m^{-2}\ h^{-1}$ for mixed clarification equipment.

Although solvent extraction has been successful in recovering essential non-ferrous metals, it faces challenges such as slow extraction, difficult phase separation, and low efficiency. Additionally, the need for sequential extraction and stripping steps, along with the use of large amounts of potentially toxic and flammable organic solvents and extractants, raises environmental and safety concerns.[25] As alternatives, emulsion liquid membrane, bulk liquid membrane, supported liquid membrane (SLM), hollow fiber renewal liquid membrane and other separation technologies have been applied in hydrometallurgy for Cu^{2+}, Co^{2+}, Ni^{2+} and Zn^{2+} recovery and separation.[26–28] However, a drawback is the loss of membrane solvent and/or carrier into the aqueous phase during prolonged processes, leading to reduced lifespan of the membranes and hindering the industrial application of membrane separation technologies.

Fortunately, polymer inclusion membranes (PIMs) offer a solution to the problem of losing membrane solvent or carrier during long processes. They come with several advantages, including high selectivity, easy preparation, and high extraction efficiency.[29–31] In the PIMs extraction, specific metal ions move through a reversible coordination–dissociation reaction between metal ions and extractants immobilized in the base polymer.[32] Studies have shown that PIMs exhibit good durability, long-term stability, and higher selectivity compared to SLMs.[33] The efficiency and selectivity of PIMs rely on the carrier used, making the choice of an appropriate carrier crucial for recovering and separating specific metal ions.[34] Recent research has identified Aliquat 336, Acorga M5640, LIX84-I and 2-aminomethylpyridineas effective extractants for removing and recovering of strategic non-ferrous metal ions.[35–38] However, understanding the intricate relationship between the microstructure and separation mechanism of PIMs remains a complex and active area of research. This complexity depends on factors such as the size of substances to be separated, the pore size of PIMs, operating conditions, and the membrane's specific material and design.[35,38]

In this study, we aim to combine solvent extraction and PIM separation technologies to create a novel PIM material designed for selectively separating and concentrating copper(II) from polymetallic acidic solutions. Our goal is to streamline the technological process, cut production costs, and enhance the separation coefficients between copper(II) and other metals. We assessed the efficiency of selectively extracting copper(II) under different H_2SO_4 concentrations in stripping solutions, extraction temperatures, and membrane components in the presence of Co^{2+}, Ni^{2+}, and Zn^{2+}. To understand the mechanism of selective separation and enrichment of copper(II) ions, we employed techniques such as Brunauer–Emmett–Teller (BET) and density functional theory (DFT) calculations.

2. Experimental

To optimize the PIM separation process, we studied the effects of H_2SO_4 concentration in the stripping solution, extraction temperature, and the components of the membrane on the efficiency of copper(II) extraction. Simultaneously, Brunauer–Emmett–Teller (BET) measurements and density functional theory (DFT) calculations were employed into the investigation of the mechanism of selective separation and enrichment of copper(II) ions.

2.1 Reagents and materials

2-Nitrophenyl-*n*-octyl ether (NPOE, Fig. 1a) and poly(vinyl) chloride (PVC) were purchased from Shanghai Aladdin Co., Ltd as utilized without additional purification. NPOE served as the plasticizer in this work to maintain the softness of the PIM membranes and enhance their mechanical strength, while PVC was used as the base material for the membranes. Mextral®5640H (Fig. 1b) functioned as an extractant/carrier and was kindly provided by Chongqing KOPPERCHEM Industry Co., Ltd (China). $CuSO_4 \cdot 5H_2O$, $NiSO_4 \cdot 6H_2O$, $ZnSO_4 \cdot 7H_2O$ and $CoSO_4 \cdot 7H_2O$ were supplied by Shanghai Aladdin Co., Ltd and used without any pretreatment. Tetrahydrofuran (THF) served as a solvent for the plasticizer and was purchased from Shanghai Aladdin Co., Ltd. Throughout the experiment, ultrapure water with a resistance of 18.2 MΩ cm, prepared using a Milli-Q System, was used.

2.2 Methods

2.2.1 Polymer inclusion membranes (PIMs) and feed solutions preparation. The solvent evaporation method[30] was utilized to create PIMs. Initially, distinct membrane components (PVC, NPOE, and Mextral®5640H) with different ratios and weighing 0.5 g in total were dissolved in 10 mL THF. These solutions were then transferred into a glass culture dish with a diameter of 6 cm. Allowing THF to slowly evaporate of at ambient temperature for 12 h resulted in flexible, colorless, and transparent membranes with robust mechanical properties, referred to as Mextral®5640H-based PIMs. Subsequently, the obtained membranes were then carefully peeled off from a glass

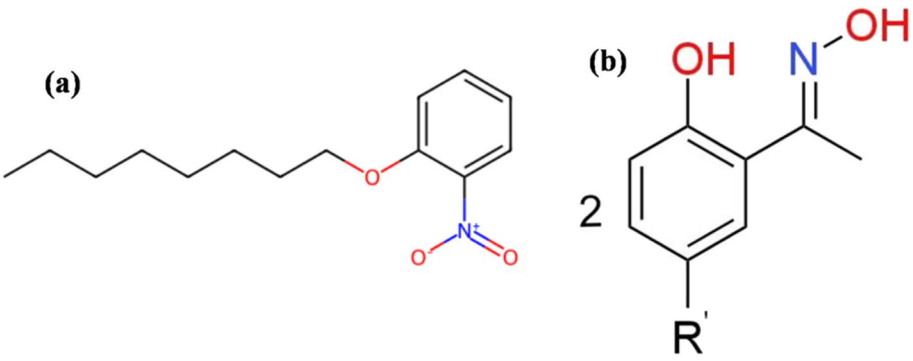

Fig. 1 The chemical structure of NPOE (a) and Mextral®5640H (b).

culture dish and stored for subsequent experiments. For the feed solutions, accurate masses of $CuSO_4 \cdot 5H_2O$, $NiSO_4 \cdot 6H_2O$, $ZnSO_4 \cdot 7H_2O$ and $CoSO_4 \cdot 7H_2O$ were weighed, dissolved in ultrapure water, and diluted to a specific volume. The pH of the resulting feed solution was adjusted to 5.0 by diluted sulfuric acid.

2.2.2 Selective extraction of metal ions. The optimization of the selective metal ion extraction process was carried out using an in-house separation apparatus depicted in Fig. 2, with an effective area of the membrane of 13.27 cm^2. In a thermostatic water bath, equal volumes (200 mL) of both the feed and stripping solutions were maintained at a constant temperature. Peristaltic pumps were employed as the power device to circulate the feed solution and stripping solution at a flow rate of 100 mL min^{-1} during the membrane extraction process. At specific one-hour intervals, 0.2 mL aliquots were transferred from the compartment of the stripping solution to determine the metal ions concentration using ICP-OES (AGILENT 725-ES, USA). The metal ion concentrations in the organic phase were determined by calculating the difference.

As depicted in Fig. 2, the feed solution containing Cu^{2+}, Co^{2+}, Ni^{2+} and Zn^{2+} was passed through the feed solution compartment. Here, the extractable metal ions were selectively transferred into the membrane matrix at the membrane/feed solution interface. This transfer occurred due to the differences in the coordination ability and stability of the coordinated complexes between Mextral®5640H and Cu^{2+}, Co^{2+}, Ni^{2+} and Zn^{2+}. Subsequently, the organometallic complexes diffused to the opposite side of the membrane surface. These complexes were further stripped with diluted sulfuric acid in the stripping solution compartment at the solid/liquid interface. Finally, Mextral®5640H in the membrane matrix was regenerated through stripping and diffused to the membrane/feed solution interface. This process allowed for the selective extraction of metal ions from the feed solution compartment, followed by continuous stripping with diluted sulfuric acid, achieving the separation of valuable metal ions using Mextral®5640H-based PIMs.

The extraction efficiency (E), distribution ratio (D), and separation coefficient (β) were calculated as follows:

$$E = \frac{C_0 - C_{aq}}{C_0} \times 100\% \quad (1)$$

$$D = \frac{C_{aq}}{C_0 - C_{aq}} \quad (2)$$

$$\beta_{1/2} = \frac{D_1}{D_2} \quad (3)$$

In these equations, C_0 (mg L^{-1}) represents the concentration of Cu^{2+}, Co^{2+}, Ni^{2+} and Zn^{2+} in the feed solution, and C_{aq} represents the concentration of these ions in the tripping solution at specific point in time, respectively.

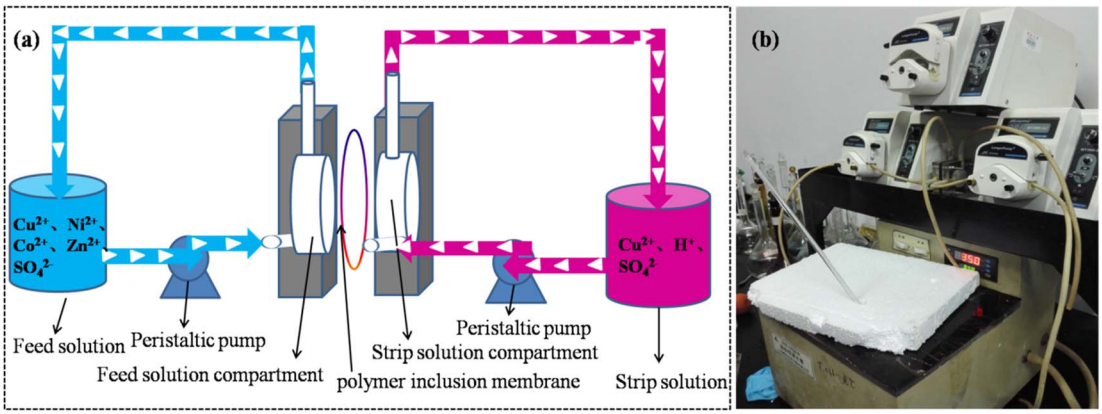

Fig. 2 The schematic diagram (a) and digital image (b) of the selective extraction apparatus.

2.2.3 Computational details. The theoretical calculations were performed using the Gaussian 16 suite of programs.[39] The structures of the studied molecules and their complexes with four metal cations (Co^{2+}, Cu^{2+}, Ni^{2+}, Zn^{2+}) were fully optimized at the PBE0-D3BJ/def2-SVP level of theory. The vibrational frequencies of the optimized structures were computed at the same level. Each structure was confirmed as a local energy minimum on the potential energy surface by verifying that all the vibrational frequencies were real.

2.2.4 Membranes characterization. The FT-IR spectra of Mextral®5640H were recorded on a Nicolet 6700 FT-IR spectrophotometer (Thermo Fisher Scientific, USA) using KBr pellets. 32 scans at a resolution of 4.0 cm^{-1} were averaged to obtain each spectrum over the wavenumber range of 400–4000 cm^{-1}. The FT-IR spectra of the membranes were recorded directly. All spectrum measurements were performed at ambient temperature. The full aperture size distribution of the membranes were determined using the Brunauer–Emmett–Teller (BET) model from nitrogen adsorption and desorption isotherms. These isotherms were measured at the temperature of liquid nitrogen on an ASAP 2460 (Mcmurretik Instrument Co., Ltd (Shanghai)) surface area analyzer with adsorption data in the relative pressure range from 0.05 to 0.995.[40,41]

3. Results and discussion

3.1 Optimization of the membrane extraction process and stability tests

3.1.1 Effects of membrane components on efficiency and selectivity of copper extraction. The efficiency and selectivity of copper extraction greatly depend on the membrane properties and the amount of carrier molecules incorporated within the membrane. The extraction of copper(II) largely depend on how it interacts with the carrier (Mextral®5640H), so, it is important to use the right amount of this carrier.[42] In the present work, we used PVC as the frame work of polymer membrane. If there is too much PVC, the mass transfer rate is reduced, but too little PVC can decrease the mechanical performance of the membrane. Therefore, we keep a mass fraction of PVC between 30 and 40%.[42] In addition, NPOE was used as the plasticizer. When its content goes above 40% (by mass), the membranes become too sticky and soft, which makes them unsuitable for selectively extraction of metal ions.[42] However, if the NPOE content is below 40%, increasing its amount does improve copper extraction efficiency. Therefore, we also keep the content of NPOE between 30 and 40%. Additionally, since the amount of carrier we can use is limited, we should keep the concentration of metal ions in the feed solution low to optimize the extraction process.

Therefore, to determine the optimal components for the efficient extraction of Co^{2+}, Cu^{2+}, Ni^{2+}, and Zn^{2+}, we varied the mass fraction of Mextral®5640H, PVC and NPOE. The amount of Mextral®5640H was kept constant at 30%, and the mass fraction of NPOE and PVC was adjusted. Fig. 3 illustrates that the Cu^{2+} extraction efficiency and membrane selectivity increased with a higher amount of NPOE plasticizer. At 40% NPOE, cooper was nearly 100% extracted, and the separation coefficients β with respect to Ni^{2+}, Zn^{2+}, and Co^{2+} were calculated to be 210 357, 98 148 and 171 904, respectively, after 7 hours of equilibration. The separation coefficients $\beta_{Cu/Ni}$ in

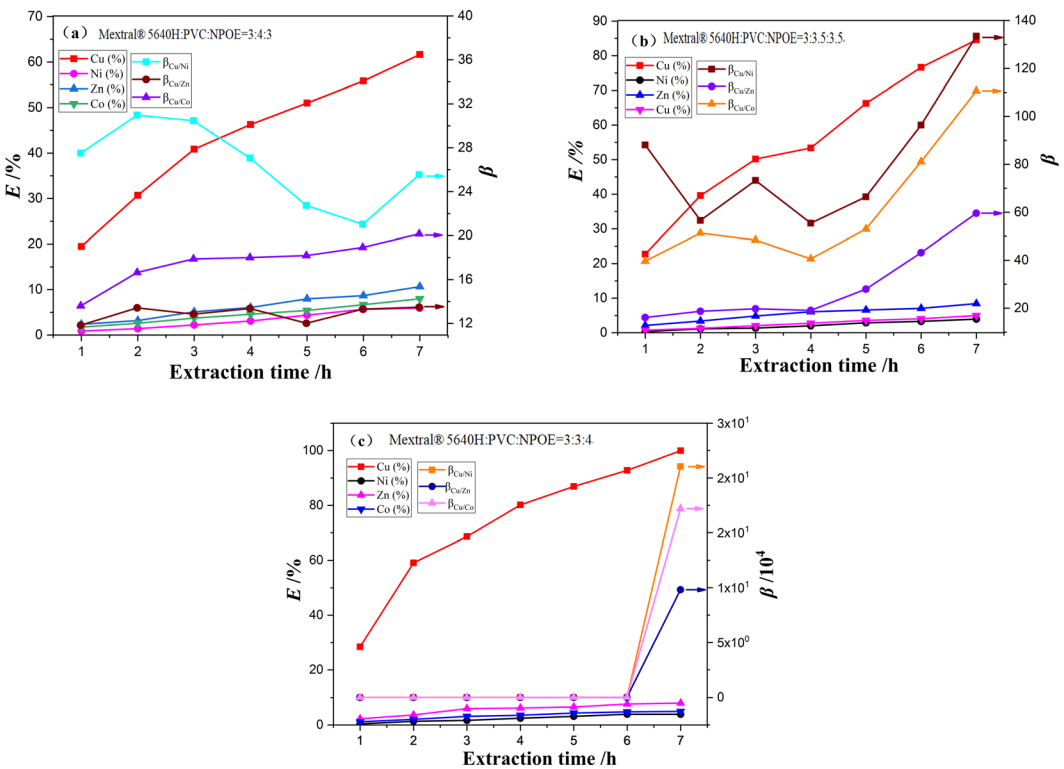

Fig. 3 The effects of membrane composition on the extraction efficiency (E) and separation coefficient (β) of PIMs.

Fig. 3a and both $\beta_{Cu/Ni}$ and $\beta_{Cu/Co}$ in Fig. 3b fluctuate slightly with the increase of extraction time. This may be due to differences in the extraction kinetics of Cu^{2+} compared with those of Ni^{2+} and Co^{2+}.[43] However, when the NPOE plasticizer exceeded 40%, the resulting PIMs became too soft and sticky, impeding the transport of extractable metal ions. Therefore, we propose the optimal mass fraction between Mextral®5640H, PVC and NPOE to be 3 : 3 : 4.

3.1.2 Effect of H_2SO_4 concentration on efficiency and selectivity of copper extraction. The back-extraction process plays an important role in the extraction of metal ions. Therefore, we investigated the impact of H_2SO_4 concentration in the stripping solutions on extraction efficiency (E) and separation coefficient (β). All extraction experiments were conducted at 25 °C with a fixed mass fraction between Mextral®5640H, PVC and NPOE at 3 : 3 : 4. Due to strong coordination and the formation of a stable complex between Mextral®5640H and Cu^{2+}, the stripping solution required relatively high concentration of H_2SO_4 to achieve an efficient back-extraction.

As depicted in Fig. 4, an increase in H_2SO_4 concentration in the stripping solution from 0.3 to 0.9 mol L^{-1} led to a rise in the extraction efficiency of Cu^{2+} after 7 hours from 40.31% to 99.98%. Simultaneously, the separation coefficient between $Cu^{2+}$and Ni^{2+}, Zn^{2+}, and Co^{2+} reached 921 255, 485 027 and 834 601, respectively. The significant fluctuations of separation coefficients occur when the H_2SO_4 concentration in the stripping solution exceeds 0.9 mol L^{-1}. These fluctuations could be attributed to the low extraction efficiency of Ni^{2+}, Zn^{2+}, and Co^{2+} in the early stage of extraction. Meanwhile, the extraction efficiency of Cu^{2+} rapidly increases with extraction time, while

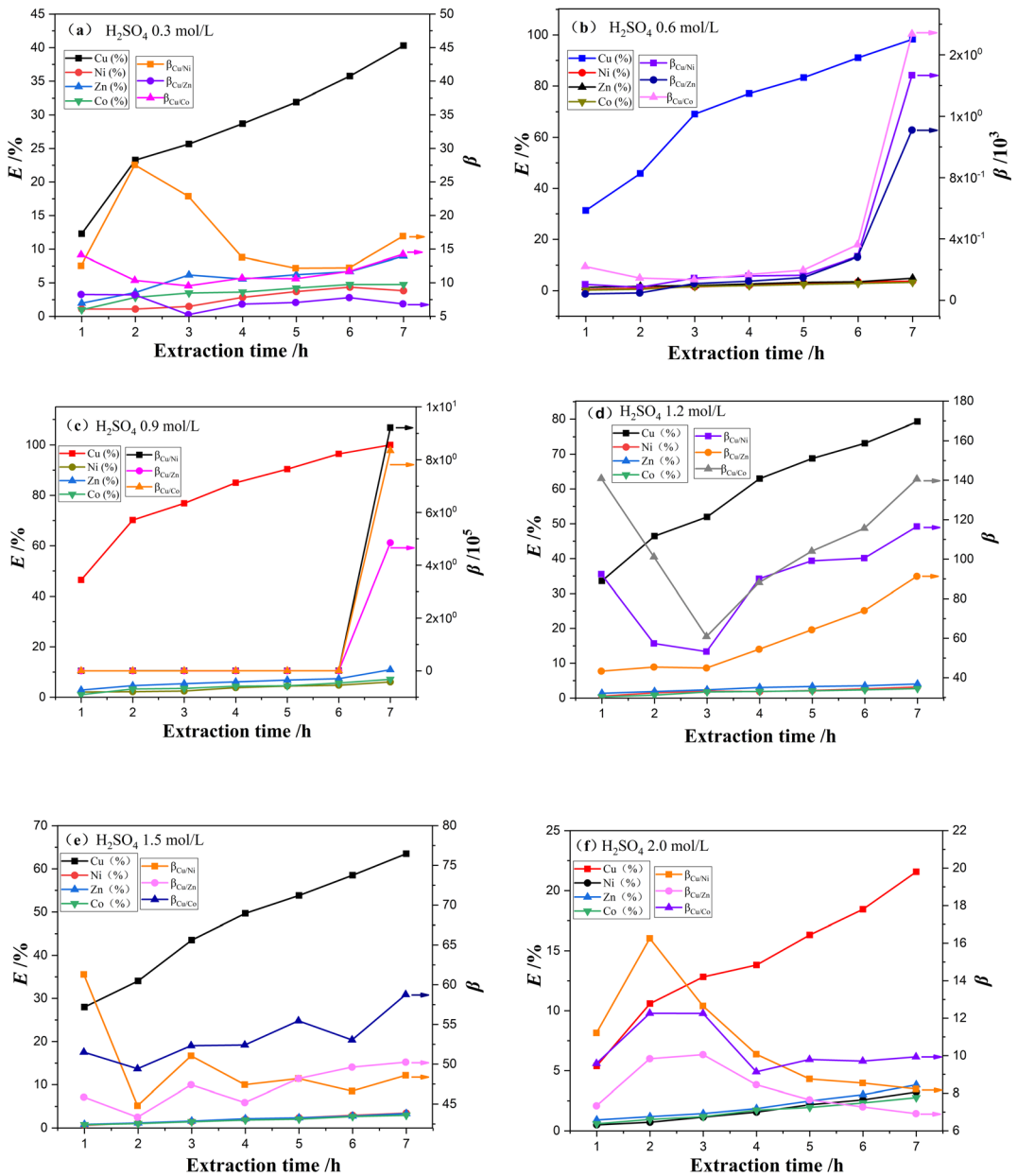

Fig. 4 The effect of H_2SO_4 concentration in the stripping solution on E and β values of four precious metal cations.

other metals are extracted negligibly. This results in high selectivity for copper extraction. However, at higher sulfuric acid concentrations, the extraction efficiency of Cu^{2+} decreased from 100% to 21.57%, while the extraction efficiency of Ni^{2+}, Zn^{2+}, and Co^{2+} reached 3.23%, 3.83% and 2.77%, resulting in a decrease in the separation coefficient between $Cu^{2+}$and Ni^{2+}, Zn^{2+}, and Co^{2+} to 8.23, 6.91 and 9.93, respectively. The lower extraction efficiency of Cu^{2+} at higher H_2SO_4 concentrations in the stripping solution can be attributed to the decreased stability of carriers incorporated into polymer inclusion membranes, while the increased extraction efficiency of Ni^{2+}, Zn^{2+}, and Co^{2+}(ref. 38) contributes to this effect. Hence, we chose 0.9 mol L^{-1} H_2SO_4 in the stripping solution for the subsequent experiments.

3.1.3 Effects of temperature on extraction efficiency and separation coefficient. Higher temperatures accelerate chemical reactions, potentially aiding the extraction of copper from the aqueous medium. Therefore, we investigated the effects of the temperature of stripping and feed solutions on the extraction efficiency (E) and separation coefficient (β). All extraction experiments were conducted with a 0.9 mol L^{-1} H_2SO_4 concentration in the stripping solution and a 3 : 3 : 4 mass fraction of Mextral®5640H, PVC and NPOE in the PIM membrane. The temperature of stripping and feed solutions was controlled between 25 and 65 °C using a thermostatic water bath.

As depicted in Fig. 5, the extraction efficiency of Cu^{2+} and separation coefficients increased significantly. The extraction efficiency of Cu^{2+} increased from 96.47% to 100%, and the

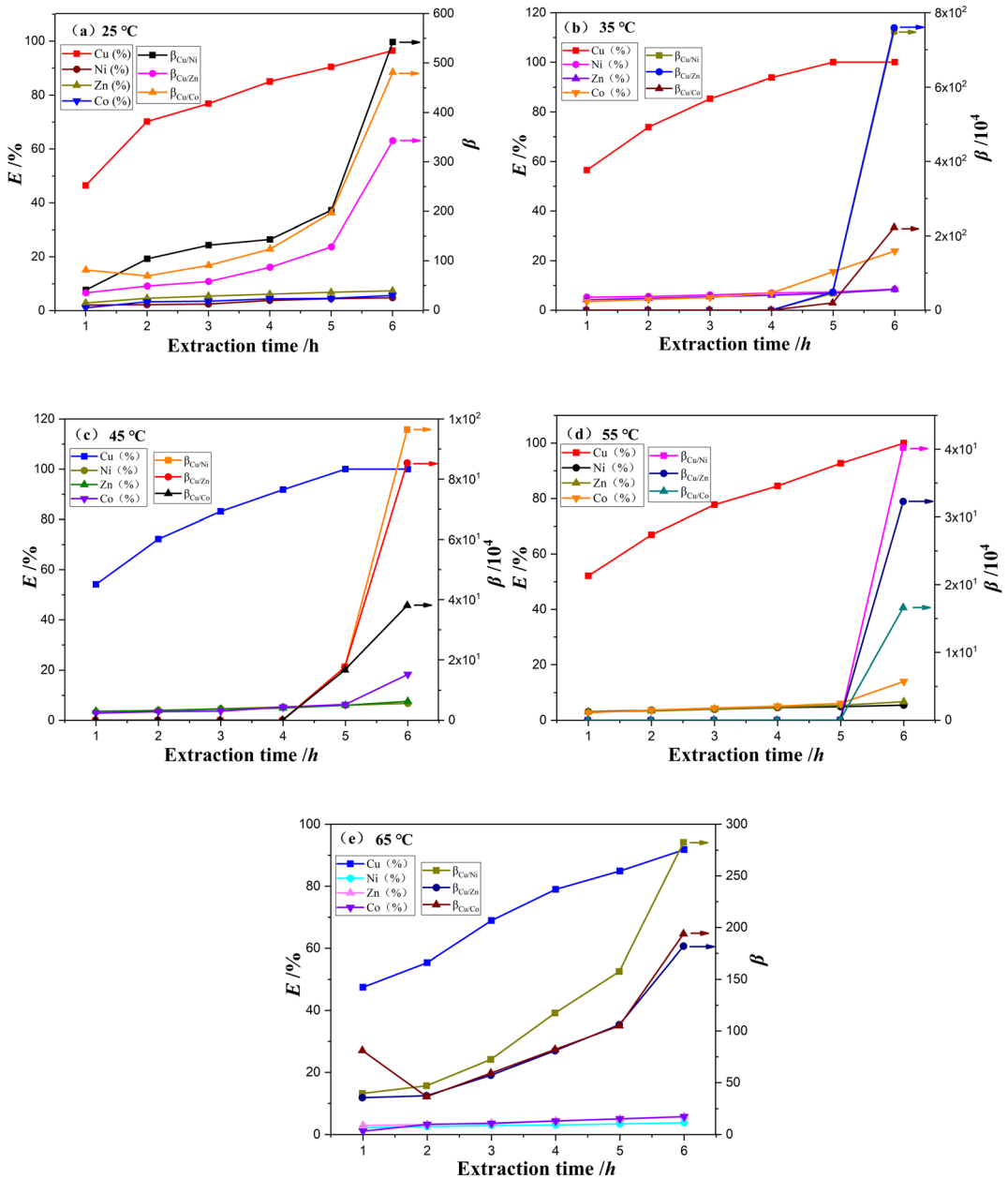

Fig. 5 The effect of temperature on the extraction efficiency (E) and separation coefficient (β).

separation coefficient between Cu^{2+} and Ni^{2+}, Zn^{2+}, and Co^{2+} increased about 10^4 times as the extraction temperature rose from 25 °C to 35 °C after 6 hours of extraction. However, with further increases in extraction temperature from 35 °C to 65 °C, the extraction efficiency of other valuable metals increased slowly, resulting in decrease in the separation coefficient between Cu^{2+} and Ni^{2+}, Zn^{2+}, and Co^{2+}. This can be attributed to the increased mass transfer rate of Ni^{2+}, Zn^{2+} and Co^{2+} at elevated temperatures and the decreased efficiency copper extraction. Therefore, the optimal extraction temperature was determined to be 35 °C.

3.1.4 Chemical stability of PIM. We next evaluated the chemical stability PIMs during the extraction process. After selectively extracting copper from acidic solutions containing multiple metals for 300 hours, no significant weakening of the mechanical properties or reduction of extraction efficiency was observed. However, with the extended extraction time, a light-green color appeared on the exposed surface of the PIM. This color may originate from the reaction of Mextral®5640H in the PIM with Cu^{2+}.[43] Washing with a dilute sulfuric acid solution, removed the color, resulting from the back extraction of Cu^{2+}.[44]

3.2 FT-IR studies of the extraction mechanism of PIMs

To understand the membrane extraction mechanism, we recorded the FT-IR spectra of the extractant (Mextral®5640H), the unloaded polymer inclusion membrane (PIM), and the PIM loaded with metal ions.

As displayed in Fig. 6, the strong vibration peaks located around 2963–2856 cm^{-1} (Fig. 6a–c) corresponded to the C–H groups of aliphatic and phenol groups in Mextral®5640H and NPOE.[45] The band at 1624 cm^{-1} (Fig. 6a) assigned to the C=N stretching vibration in Mextral®5640H shifted to 1608 cm^{-1} (Fig. 6b) due to interactions between Mextral®5640H and NPOE. Furthermore, the interaction between the Mextral®5640H oxime group with metal ions induced a more pronounced peak shift to 1582 cm^{-1} (Fig. 6c).[30,45] The absorption peak at 1384 cm^{-1} originating from the deformation vibration of the phenolic –O–H group in Mextral®5640H disappeared in PIMs (Fig. 6b and c) due to intermolecular hydrogen-bonding with the plasticizer.[45] The vibration band at 3398 cm^{-1} (Fig. 6a), attributed to –OH stretching vibrations of the extractant, was preserved in the unloaded PIM (Fig. 6b). However, the peak broadened and shifted to 3405 cm^{-1} due to hydrogen-bonding between Mextral®5640H and NPOE. This peak disappeared in the loaded PIM (Fig. 6c) due to the coordination of the extractant with metal ions, which disrupted the inter- and intramolecular hydrogen bonding of Mextral®5640H.[30,45] Additional FT-IR peaks observed at 1161 cm^{-1}, 1353 cm^{-1} and1527 cm^{-1} were attributed to C–O–C, C–N, and C–NO_2 groups of NPOE (Fig. 6b and c).[45] Considering all these results, we propose the structure of extracted complexes as displayed in Fig. 7, where M represents Cu^{2+}, Ni^{2+}, Co^{2+} and Zn^{2+}, respectively.

3.3 Pore size distribution of unloaded PIM

The microstructure of membranes, including factors like pore size, distribution, and membrane thickness, plays a pivotal role

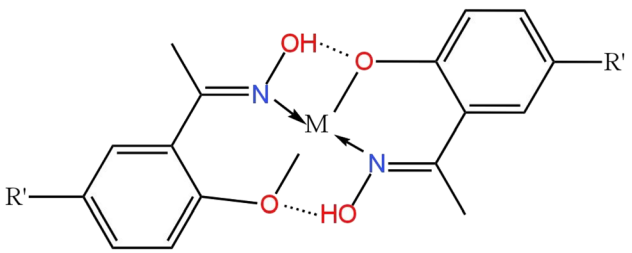

Fig. 7 The plausible structure of the extracted complexes. M represents Cu, Ni, Co, or Zn ions.

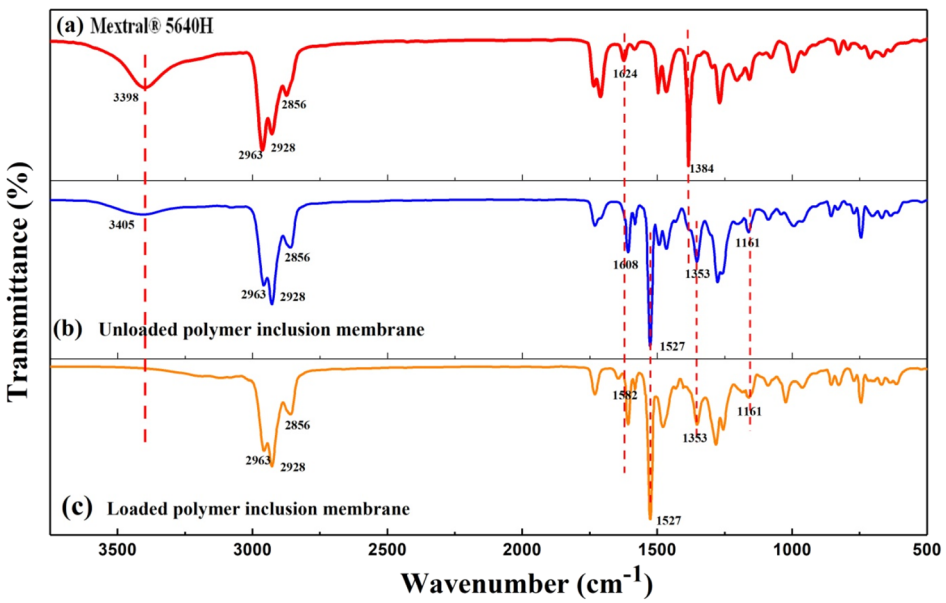

Fig. 6 FT-IR spectra of Mextral®5640H (a), unloaded PIM (b), and loaded PIM (c).

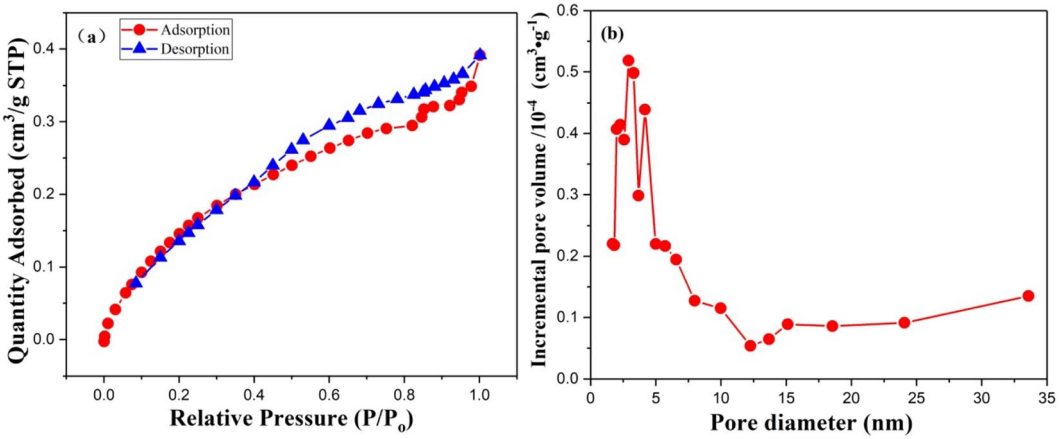

Fig. 8 BET isotherms (a) and pore size distribution (b) of unloaded PIM.

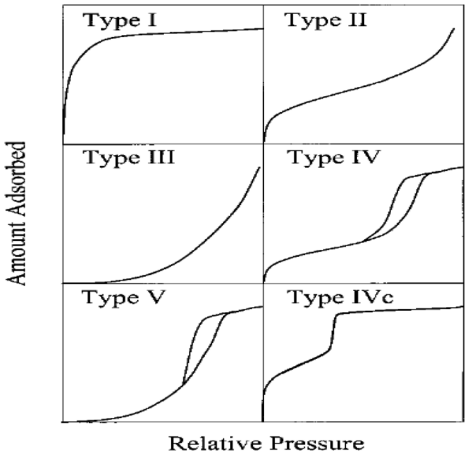

Fig. 9 Classification of gas adsorption isotherms.[46]

in their separation performance. These characteristics are particularly important in processes like microfiltration and ultrafiltration, where separation is mainly determined by pore size. Larger substances are retained while smaller substances pass through, highlighting the crucial role of microstructure in the separation mechanism. In this context, we utilized the BET model based on nitrogen adsorption and desorption isotherms to investigate the pore size of the PIM. The analyzed sample consisted of a membrane synthesized under optimum composition for maximizing extraction yield, *i.e.* 3 : 4 : 3 mass ratio of Mextral®5640H, NPOE and PVC. The results are shown in Fig. 8.

The gas adsorption isotherms presented in Fig. 9 indicate a type IV isotherms, as illustrated in Fig. 7a. Moreover, examining the hysteresis loops and their corresponding pore shapes (Fig. 10) classifies ring the PIM membrane's hysteresis ring (Fig. 8a) as type A. A smaller hysteresis ring suggests relatively high membrane porosity, characterized by cylindrically-shaped pores. Fig. 8b illustrates that the majority of the membrane pores have diameters ranging from 2.0 to 5.0 nm. The calculated average pore diameter is 3.2686 nm, with numerous pores larger exceeding 3.5 nm. If pore size significantly influences extraction efficiency and separation coefficient, the diameter of the Cu^{2+}–Mextral®5640H complex should be smaller than the average pore size. Conversely, complexes of the other three metal cations (Ni^{2+}, Zn^{2+}, and Co^{2+}) with the extractant should be larger than the membrane's pore size.

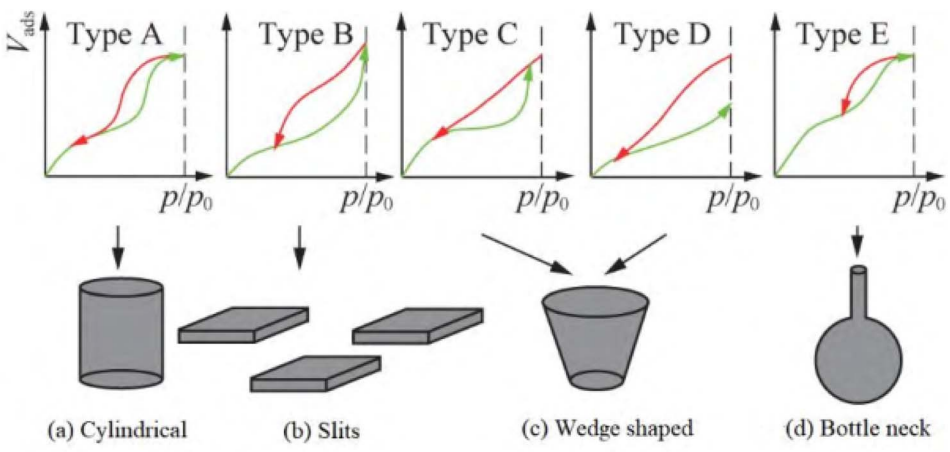

Fig. 10 Classification of hysteresis loops of adsorption isotherms and their corresponding pore shapes.[46]

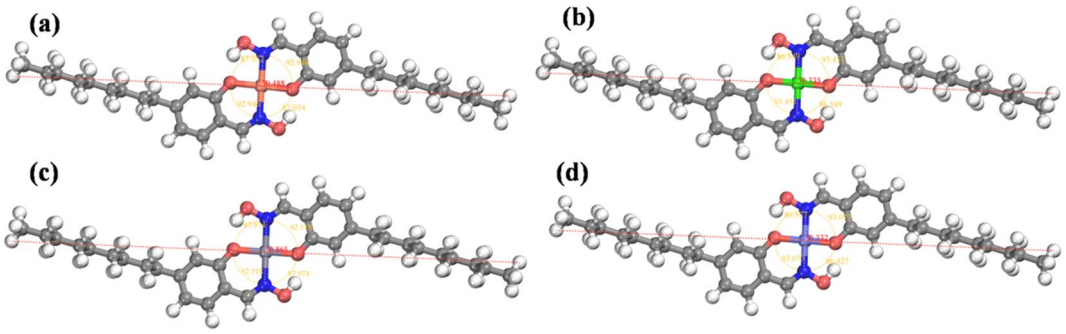

Fig. 11 The optimized geometry and molecular size of the extractant-metal ion complexes for Cu (a), Ni (b), Zn (c), and Co (d).

Table 1 The total energy, interaction energy, and molecular size of complexes of each of the four metal cations with the extractant

System	Energy/Hartree	Interaction energy/Hartree	Interaction energy/kcal mol^{-1}	Molecular size/Å
Mextral®5640H + Cu^{2+}	−3038.12450	−0.05255	−32.97756	30.448
Mextral®5640H + Ni^{2+}	−3163.64661	−0.10503	−65.90732	30.335
Mextral®5640H + Zn^{2+}	−3434.72654	−0.03891	−24.41724	30.865
Mextral®5640H + Co^{2+}	−3295.79823	−0.04226	−26.51646	30.332

3.4 Structural analysis of the extractant-metal ion complexes

The metal extraction experiments revealed a significant difference in the extraction performance of PIMs toward Cu^{2+} compared with Ni^{2+}, Zn^{2+}, and Co^{2+}. To gain more insights into the structural basis of this trend, we optimized the structures of the four hypothesized coordination compounds to obtain information on their molecular size and stability. The results of quantum chemical calculations are illustrated in Fig. 11 and summarized in Tables 1 and 2.

Evidently, the sizes of all four organometallic compounds, ranging from 30.3 to 30.9 Å, were smaller than the average pore diameter (3.2686 nm). This implies that molecular size is not the main factor influencing the separation mechanism of these metal cations. The calculated potential energies for the four complexes (Table 1) highlighted that the complex with Cu^{2+} ions has the largest overall energy, *i.e.* the lowest stability, which is beneficial for the back-extraction of Cu^{2+}–Mextral®5640H complex. The enthalpy and entropy of the reaction as well as Gibbs free energy of the complexes shown in Table 2 indicate that the complex with Cu^{2+} has lower stability compared to those with Ni^{2+}, Zn^{2+}, and Co^{2+}. As discussed in Section 3.1.2, the increased acid concentration in the stripping solution improved the extraction of Ni^{2+}, Zn^{2+}, and Co^{2+} and thereby reduced the separation coefficients. The results of theoretical calculations support these results, as more stable complexes correlate with lower extraction rates and poorer extraction performance. Therefore, the stability and back-extraction performance played a significant role in the selective extraction of copper from the feed solution.

Table 2 Enthalpy, Gibbs free energy and entropy- of the formation of metal extractant complexes

System	ΔH/kcal mol^{-1}	ΔG/kcal mol^{-1}	ΔS/cal K^{-1}
Mextral®5640H + Cu^{2+}	−23.801075	−7.60787345	−0.054339603
Mextral®5640H + Ni^{2+}	−27.3597875	−13.4705002	−0.046608347
Mextral®5640H + Co^{2+}	−37.22597	−21.8255475	−0.05167927
Mextral®5640H + Zn^{2+}	−40.56427	−26.76592875	−0.046303159

4. Conclusions

In summary, our study proposes an innovative integration of solvent extraction and PIM membrane separation technology to fabricate a novel PIM membrane material. This material demonstrates efficient and selective separation and enrichment of strategic valuable metals, particularly copper(II), from polymetallic acidic solutions. We systematically explored the impact of PIM composition, extraction temperature, and H_2SO_4 concentration in the stripping solution on extraction and separation performance.

The optimization process identified the ideal extraction conditions as a mass fraction of Mextral®5640H : PVC : NPOE = 3 : 3 : 4, extraction temperature at 35 °C, and 0.9 mol L^{-1} H_2SO_4 in the stripping solution. Under these conditions, we achieved impressive extraction efficiencies of 100% for Cu^{2+}, 8.53% for Ni^{2+}, 8.43% for Co^{2+}, and 23.89% for Zn^{2+}.

To explain the substantial variation in extraction performance between Cu and the other metals, we employed the comprehensive approach. The FT-IR spectra, BET analysis, and theoretical calculations provided crucial structural insights, including molecular size and potential energy, for copper and the other metal-ion extracted complexes within the PIM. The results underscored that all the extracted complexes molecular could pass through the PIMs in terms of molecular size. Hence, stability and back-extraction performance were identified as

crucial for the selective extraction of copper with respect to the other three metal ions. The success of this synergistic approach lays the foundation for advancements in the field of metal separation technologies. Future research directions could be oriented towards scaling up this methodology for industrial applications, with a focus on optimizing process parameters for enhanced efficiency and environmental sustainability.

Conflicts of interest

There are no conflicts to declare.

Acknowledgements

This work was financially supported by Basic Research Project of Key Field Project of Natural Science Research of Guizhou Provincial Department of Education (Qian Jiao He KY Zi [2020] 049), Scientific Research (Cultivation) Project of Liupanshui Normal University (LPSSY2023KJZDPY05), Liupanshui Science and Technology Project (52020-2023-0-2-17), Carbon Neutral Engineering Research Center of Guizhou colleges and universities in Coal Industry (Qian Jiao Ji [2023]044), Guizhou Province first-class professional construction point (GZSylzy202103) and Innovation Team Foundation of Education of Guizhou Province (Qian Jiao Ji [2023]087).

Notes and references

1 Z. H. Liu, Present situation and development of non ferrous metallurgy technology, *World Nonferrous Metals*, 2020, (12), 13–14.
2 China Nonferrous Metals Industry Association, *China Nonferrous Metals Industry Year Book*, China Nonferrous Metals Industry Association, Beijing, 2014.
3 R. H. Lin, The current situation and prospects of the development of non-ferrous metal mineral resources in China, *China Metal Bulletin*, 2011, (35), 2–7.
4 R. G. Cui, S. C. Liu, J. Guo, *et al.*, The characteristics of the situation of mineral resources in China in 2012, *China Mining Magazine*, 2013, **22**(1), 1–4.
5 L. G. Meng and Z. Q. Sun, Development of Mineral Resources and Sustainable Development, *Mod. Min.*, 2010, (10), 10–12.
6 X. Li, B. Li, S. Wu, *et al.*, Silica-Based 2-Aminomethylpyridine Functionalized Adsorbent for Hydrometallurgical Extraction of Low-Grade Copper Ore, *Ind. Eng. Chem. Res.*, 2012, **51**(46), 15224–15232.
7 B. Pospiech, Synergistic Solvent Extraction and Transport of Zn(II) and Cu(II) across Polymer Inclusion Membranes with a Mixture of TOPO and Aliquat 336, *Sep. Sci. Technol.*, 2014, **49**(11), 1706–1712.
8 J. T. Li and A. L. Chen, Deep removal of copper from nickel electrolyte using manganese sulfide, *Trans. Nonferrous Met. Soc. China*, 2015, **25**(11), 3802–3807.
9 X. Qiu, H. Hu, J. Yang, *et al.*, Selective removal of copper from simulated nickel electrolyte by polystyrene-supported 2-aminomethylpyridine chelating resin, *Chem. Pap.*, 2018, **72**(8), 2071–2085.
10 L. Bai, H. Hu, W. Zhang, *et al.*, Amine/acid catalyzed synthesis of a new silica-aminomethyl pyridine material as a selective adsorbent of copper, *J. Mater. Chem.*, 2012, **22**(33), 17293–17301.
11 M. Fu, J. Hu, Y. Li, *et al.*, A novel strategy achieving enrichment of metal values from and into ammoniacal solutions, *Sep. Purif. Technol.*, 2015, **151**, 97–101.
12 X. Wu, S. Zhu and S. Li, Synergistic Extraction Mechanism of Versatic10 and LIX63 for Ni^{2+}, Co^{2+}, Mn^{2+}, *Hydrometallguty*, 2020, **39**(01), 34–40.
13 S. Zhu, H. Hu, S. Li and C. Wang, The application of structural analysis in the investigation of solvent extraction mechanism, *J. Coord. Chem.*, 2022, **5–6**(75), 549–572.
14 W. Zhang, C. Y. Cheng, M. Rodriguez, *et al.*, Separation of copper, iron and zinc from cobalt and nickel with mixed Cyanex 272 and LIX84 extractants, in *Proceedings International Solvent Extraction Conference ISEC*, 2008, vol. 1, pp. 177–182.
15 C. Y. Cheng, W. Zhang and Y. Pranolo, Separation of Cobalt and Zinc from Manganese, Magnesium, and Calcium Using a Synergistic Solvent Extraction System Consisting of Versatic 10 and LIX 63, *Solvent Extr. Ion Exch.*, 2010, **28**(5), 608–624.
16 D. Dreisinger, C. Y. Cheng, W. S. Zhang, *et al.*, Development of the Boleo process flowsheet and the Direct Solvent Extraction (DSX) circuit for cobalt and zinc recovery, in *Proceedings XXV International Mineral Processing Congress*, 2010, pp. 309–317.
17 C. Y. Cheng, K. R. Barnard, W. Zhang, *et al.*, Synergistic Solvent Extraction of Nickel and Cobalt: A Review of Recent Developments, *Solvent Extr. Ion Exch.*, 2011, **29**(5–6), 719–754.
18 S. Zhu, H. Hu, J. Hu, *et al.*, Insights into the extraction mechanism from the coordination chemistry of copper(II) with a synergistic mixture which mimics Versatic10 and 2-ethylhexyl 4-pyridinecarboxylate ester, *J. Coord. Chem.*, 2017, **19**(70), 3325–3337.
19 S. Zhu, H. P. Hu, J. Y Li, F. Hu, *et al.*, The Coordination Structure of the Extracted Nickel(II) Complex with a Synergistic Mixture Containing Lix63 and Versatic10, *J. Chin. Chem. Soc.*, 2017, **64**, 205–216.
20 C. Y. Cheng, G. Boddy, W. Zhang, *et al.*, Recovery of nickel and cobalt from laterite leach solutions using direct solvent extraction: part 2: semi- and fully-continuous tests, *Hydrometallurgy*, 2010, **104**(1), 53–60.
21 C. Y. Cheng, M. D. Urbani, M. G. Davies, *et al.*, Recovery of nickel and cobalt from leach solutions of nickel laterites using a synergistic system consisting of Versatic 10 and Acorga CLX 50, *Miner. Eng.*, 2015, **77**, 17–24.
22 C. Y. Cheng, K. R. Barnard, W. Zhang, *et al.*, Recovery of nickel, cobalt, copper and zinc in sulphate and chloride solutions using synergistic solvent extraction, *Chin. J. Chem. Eng.*, 2016, **24**(2), 237–248.
23 Z. Zhu, W. Zhang, Y. Pranolo, *et al.*, Separation and recovery of copper, nickel, cobalt and zinc in chloride solutions by synergistic solvent extraction, *Hydrometallurgy*, 2012, **127–128**(18), 1–7.

24 J. Y. Li, *Study on the Selective Extraction of Nickel from Acid Leach Liquor of Laterite Nickel Ore and Its Synergistic Extraction Mechanism*, Central South University, Changsha, 2017.

25 D. Wang, Q. Chen, J. Hu, *et al.*, High Flux Recovery of Copper(II) from Ammoniacal Solution with Stable Sandwich Supported Liquid Membrane, *Ind. Eng. Chem. Res.*, 2015, **54**(17), 4823–4831.

26 M. Baczyńska, M. Waszak, M. Nowicki, *et al.*, Characterization of Polymer Inclusion Membranes (PIMs) Containing Phosphonium Ionic Liquids as Zn(II) Carriers, *Ind. Eng. Chem. Res.*, 2018, **57**(14), 5070–5082.

27 X. Lin, J. Tang, Y. Liu, *et al.*, Membrane-assisted enrichment of zinc(II) from and into ammoniacal media through non-dispersive synergistic extraction, *Sep. Purif. Technol.*, 2019, **210**, 268–275.

28 A. Yadollahi, M. Torab-Mostaedi, K. Saberyan, *et al.*, Intensification of zirconium and hafnium separation through the hollow fiber renewal liquid membrane technique using synergistic mixture of TBP and Cyanex-272 as extractant, *Chin. J. Chem. Eng.*, 2019, **27**(8), 1817–1827.

29 H. Duan, X. Yuan, Q. Zhang, *et al.*, Separation of Ni^{2+} from ammonia solution through a supported liquid membrane impregnated with Acorga M5640, *Chem. Pap.*, 2017, **71**(3), 597–606.

30 D. Wang, J. Hu, D. Liu, *et al.*, Selective transport and simultaneous separation of Cu(II), Zn(II) and Mg(II) using a dual polymer inclusion membrane system, *J. Membr. Sci.*, 2016, **524**, 205–213.

31 T. Tasaki, T. Oshima and Y. Baba, Selective extraction and transport of copper(II) with new alkylated pyridinecarboxylic acid derivatives, *Talanta*, 2007, **73**(2), 387–393.

32 M. I. G. S. Almeida, R. W. Cattrall and S. D. Kolev, Recent trends in extraction and transport of metal ions using polymer inclusion membranes (PIMs), *J. Membr. Sci.*, 2012, **415–416**, 9–23.

33 R. Tayeb, C. Fontas, M. Dhahbi, *et al.*, Cd(II) transport across supported liquid membranes (SLM) and polymeric plasticized membranes (PPM) mediated by Lasalocid A, *Sep. Purif. Technol.*, 2005, **42**(2), 189–193.

34 M. Ulewicz and E. Radzyminska-Lenarcik, Supported Liquid (SLM) and Polymer Inclusion (PIM) Membranes Pertraction of Copper(II) from Aqueous Nitrate Solutions by 1-Hexyl-2-Methylimidazole, *Sep. Sci. Technol.*, 2012, **47**(9), 1383–1389.

35 R. Vera, L. Gelde, E. Anticó, *et al.*, Tuning physicochemical, electrochemical and transport characteristics of polymer inclusion membrane by varying the counter-anion of the ionic liquid Aliquat 336, *J. Membr. Sci.*, 2017, **529**, 87–94.

36 F. J. Alguacil, F. A. Lopez and I. Garcia-Diaz, Copper removal from acidic wastewaters using 2-hydroxy-5-nonylbenzaldehyde oxime as ionophore in pseudo-emulsion membrane with strip dispersion (PEMSD) technology, *J. Ind. Eng. Chem.*, 2012, **18**(1), 255–259.

37 D. Wang, J. Hu, Y. Li, *et al.*, Evidence on the 2-nitrophenyl octyl ether (NPOE) facilitating copper(II) transport through polymer inclusion membranes, *J. Membr. Sci.*, 2016, **501**, 228–235.

38 J. P. Yang, H. P. Hu, Z. Y. Cheng, *et al.*, Structural insights into the coordination and selective extraction of copper(II) by tertiary amine ligands derived from 2-aminomethylpyridine, *Polyhedron*, 2017, **128**, 76–84.

39 M. J. Frisch, G. W. Tnucks, H. B. Schlegel, *et al.*, *Gaussian 16 Revision A.03*, Gaussian Inc., Wallingford, CT, 2016.

40 L. Zhang, L. Lin, Y. Zhang, *et al.*, Nickel catalysts supported on MgO with different specific surface area for carbon dioxide reforming of methane, *J. Energy Chem.*, 2014, **23**(1), 66–72.

41 X. Li, L. Jiang, C. Zhou, *et al.*, Integrating large specific surface area and high conductivity in hydrogenated $NiCo_2O_4$ double-shell hollow spheres to improve supercapacitors, *NPG Asia Mater.*, 2015, **7**(3), 165–172.

42 D. Wang, R. W. Cattrall, J. Li, *et al.*, A poly(vinylidene fluoride-co-hexafluoropropylene) (PVDF-HFP)-based polymer inclusion membrane (PIM) containing LIX84I for the extraction and transport of Cu(II) from its ammonium sulfate/ammonia solutions, *J. Membr. Sci.*, 2017, (542), 272–279.

43 Z. Y. Zhu, W. S. Zhang, Y. Pranolo, *et al.*, Separation and recovery of copper, nickel, cobalt and zinc in chloride solutions by synergistic solvent extraction, *Hydrometallurgy*, 2012, **127–128**, 1–7.

44 D. Wang, J. Hu, D. Liu, *et al.*, Selective transport and simultaneous separation of Cu(II), Zn(II) and Mg(II) using a dual polymer inclusion membrane system, *J. Membr. Sci.*, 2017, **524**, 205–213.

45 L. V. Daimay, B. C. Norman, G. F. William, *et al.*, *The Handbook of Infrared and Raman Characteristic Frequencies of Organic Molecules*, Academic Press, New York, 1991.

46 S. Zhu, J. Hu, C. Zhang, S. Li and N. An, Study on optimization and mechanism of mechanical activation process of titanium-bearing blast furnace slag, *J. Mater. Res. Technol.*, 2022, **19**, 3130–3144.